
Experimental Verification of Deposition Models for Automotive Painting with Electrostatic Rotating Bell Atomizers

David C. Conner, Prasad N. Atkar, Alfred A. Rizzi, and Howie Choset

Carnegie Mellon University, Pittsburgh, PA 15213, USA

Abstract. This paper documents the development, validation, and refinement of analytic deposition models for automotive spray painting, based largely on experimental work conducted in conjunction with the Ford Motor Company. This work, part of a larger ongoing collaborative effort with the Ford Motor Company, has the goal of developing practical and efficient trajectory planning tools for automotive painting. Our efforts thus far have led to the development of analytic deposition models for the widely used electrostatic rotating bell (ESRB) atomizers. Unlike earlier trajectory planning tools, which rely on conventional deposition models that do not capture the complexity of deposition patterns generated by ESRB atomizers, the models presented in this paper take into account both the surface curvature and the deposition pattern of ESRB atomizers. These deposition models enable our planning tools to evaluate trajectories with respect to several measures of quality, such as coating uniformity.

1 Introduction

The application of automotive paint is predominately performed by industrial robots. Unlike the largely robotic task of applying paint, the task of generating trajectories for the robots is largely a human endeavor. The specification of these trajectories by experienced technicians cannot be finished until the body design is finalized, thereby representing a major bottleneck in the concept-to-customer time line. Our research focuses on developing tools to automate the generation of these trajectories based on CAD models of the vehicle surface; thereby decreasing the amount of time required to generate the trajectories. In this paper, we describe the experimental process used to validate and refine the deposition models developed during the first phase of our research. Using these results, we will find methods to automate the task of planning trajectories given the complicated deposition patterns generated by electrostatic rotating bell atomizers (ESRB).

2 Prior Work

Automotive coating processes are moving increasingly towards the use of ESRB atomizers, shown schematically in Figure 1, in order to increase transfer efficiencies [1–3]. In an ESRB atomizer, paint fluid is forced onto the inner

surface of a high speed rotating bell [1,2]. The bell is maintained at a high voltage of 40-90 kV relative to the grounded surface being painted. Negative polarities are typically used for painting applications [4]. The paint flow breaks up at the edge of the bell, forming a cloud of droplets, as it is expelled radially due to centrifugal force imparted to the paint by the rotating bell. During this process, the electrostatically charged bell imparts a charge to each paint droplet. Both high velocity shaping air and a charged pattern control ring are used to force the charged droplets towards the grounded surface.

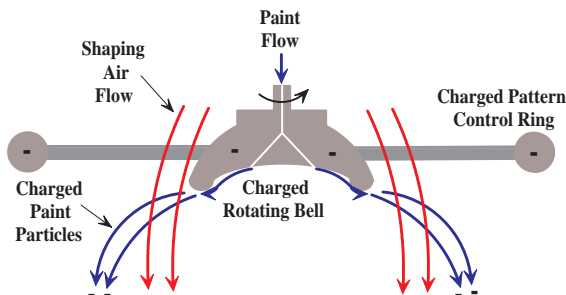


Fig. 1. Electrostatic rotating bell atomizer with paint particle trajectory and shaping air flow lines shown.

Researchers developing models of the deposition of paint by ESRB atomizers have generally focused on electrostatic effects, such as the interaction between the electric fields and the charged paint droplets, and not on the effects of various surface shapes. Early work in modeling the electrical effects of these ESRB systems was performed by Elmoursi [2], and later expanded by Ellwood and Braslaw to include coupling between the droplet flow and the electrical field [1].

The complexity of ESRB atomizer deposition patterns does not allow the use of previously developed trajectory planners. These planners have generally assumed simple deposition patterns or required the user to specify information about the deposition pattern [5–9]. Other trajectory planning research assumes the use of aerosol atomizers, which generate deposition patterns that are not compatible with the patterns generated by ESRB atomizers [10,11]. Arikan and Balkan developed a paint deposition simulation where the paint deposition model used a beta distribution [10]. Hertling *et al.* proposed more realistic deposition models for use in their trajectory planning system, but specifically limited their work to aerosol sprays citing the inherent complexity of electrostatic deposition patterns [11].

3 Deposition Modeling

The deposition models we developed represent a compromise between two fundamentally opposed evaluation criteria. First, the model must capture the

structure of the deposition to accurately predict the deposition onto a variety of surface shapes. However, the model must be computationally efficient, since it is also needed by the planner. The models we have developed attempt to balance the need for accuracy with the need for simplicity.

For the ESRB atomizers studied in this paper, the overall shape of the deposition pattern is roughly circular when the bell is oriented normal to a flat panel and the atomizer is stationary; we refer to this as the *2D deposition pattern*. As the bell moves relative to the surface, the 2D deposition pattern moves over the surface and paint is accumulated on the surface. The resulting paint thickness profile, which we refer to as the *1D collapse*, is equivalent to that obtained by integrating the deposition model along the direction of travel. Figure 2 shows the relationship between the 2D deposition pattern and the resulting 1D collapse generated by the motion of the atomizer.

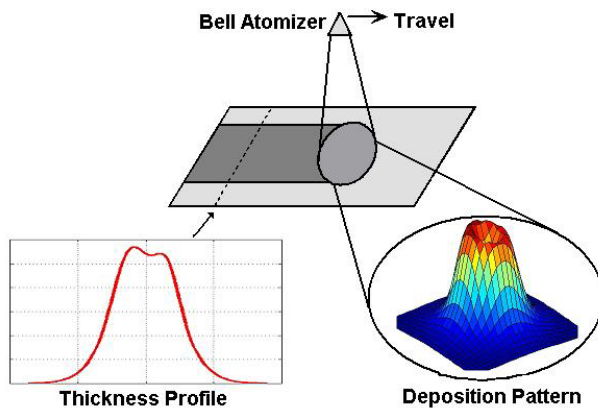


Fig. 2. Painting a flat panel: This shows the relationship between the 2D deposition pattern and the integrated thickness profile (1D collapse).

Since parameterizing the deposition model for arbitrary surfaces is difficult at best, and since experimental data for planar surfaces is readily available, we developed an analytic model for the 2D deposition pattern on a planar surface orthogonal to the orientation of the atomizer. The planar deposition is then mapped onto an arbitrary surface in a way that preserves the total paint volume. The planar surface, located at a constant distance from the atomizer, is referred to as the *deposition model plane*. The planar deposition model, $d : \mathbb{R}^2 \rightarrow \mathbb{R}$, uses two Gaussians—one offset 1D Gaussian revolved around the origin and one 2D centered Gaussian—and a scaling function that generates an asymmetry in the model. The resulting planar deposition model, similar to the asymmetric volcano shown in Figure 2, is given by

$$d(x, y) = K_1 \left((1 - K_2) f(x, y) g_1(x, y) + K_2 g_2(x, y) \right), \quad (1)$$

where $K_2 \in [0, 1]$ weights the revolved Gaussian against the centered Gaussian. To account for asymmetry in the deposition pattern, the revolved offset

Gaussian, $g_1 : \mathbb{R}^2 \rightarrow \mathbb{R}$, is scaled by the function $f : \mathbb{R}^2 \rightarrow \mathbb{R}$. We define f to be

$$f(x, y) = (1 + K_3 \sin(\text{atan2}(y, x) - \phi)),$$

where $K_3 \in [0, 1]$ weights the asymmetry scaling function for the revolved Gaussian. The phase angle, ϕ , allows the asymmetry to be localized relative to the atomizer reference frame. $K_1 \in \mathbb{R}^+$ scales the distribution to give the paint deposition flux in units of thickness per second.

Looking at the individual components of (1), the revolved offset Gaussian, g_1 , is defined to be

$$g_1(x, y) = \frac{1}{\gamma} \left(\exp \left(-\frac{(\sqrt{x^2 + y^2} - r)^2}{2\sigma_1^2} \right) + \exp \left(-\frac{(\sqrt{x^2 + y^2} + r)^2}{2\sigma_1^2} \right) \right),$$

where r is the offset radius, σ_1 is the standard deviation of the Gaussian, and γ normalizes the deposition such that integral of g_1 over x and y equals one. The centered Gaussian, $g_2 : \mathbb{R}^2 \rightarrow \mathbb{R}$, also normalized, is given by

$$g_2(x, y) = \frac{1}{2\pi\sigma_2^2} \exp \left(-\frac{x^2 + y^2}{2\sigma_2^2} \right),$$

where σ_2 is the standard deviation of the centered Gaussian.

The analytic planar deposition model, together with the mapping to arbitrary surfaces, is referred to as the *2D deposition model*, or simply the *deposition model*. The 2D deposition model, denoted $D(s, p)$, is of the form $D : \{\mathbb{R}^3 \times \mathbf{S}^2\} \times \text{SE}(3) \rightarrow \mathbb{R}$. The deposition model assigns the rate of paint deposition or *deposition flux* at a given point and surface normal, denoted $s \in \{\mathbb{R}^3 \times \mathbf{S}^2\}$, on an arbitrary surface, given $p \in \text{SE}(3)$, the location and orientation of the bell atomizer. A differential element on the deposition model plane gives a paint solids volume of $V = d(q) dx dy$, where $d(q)$ is the deposition flux at point $q = (x, y)$ on the deposition model plane. As this differential element is projected onto the surface about point s , as shown in Figure 3, the total volume must remain unchanged in order to preserve mass (assuming constant solids density). From differential geometry, it follows that $D(s, p)$ is given by

$$D(s, p) = \frac{\Omega^2 \langle \mathbf{e}, \mathbf{n} \rangle}{L^2 \langle \mathbf{e}, \mathbf{z} \rangle^3} d(q). \quad (2)$$

The reader is referred to [12] for a detailed derivation of this result.

It is also desired to have a model to predict the integrated paint deposition as the atomizer moves across a surface. Unfortunately, the complexity of the analytic 2D deposition model renders the calculation of an analytic integral intractable. Instead, we directly define the 1D collapse model using three separate Gaussians. Two Gaussians are offset from the centerline to

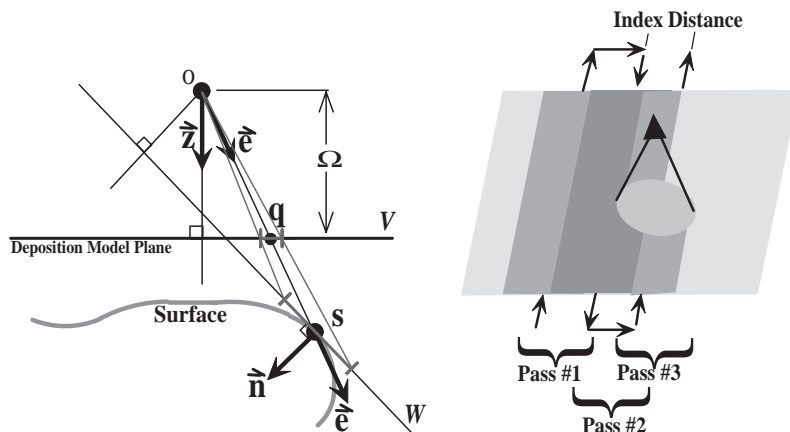


Fig. 3. (l) 2D representation of the projection of the planar deposition onto an arbitrary surface. (r) Flat panel being covered with three passes.

allow asymmetries in the deposition pattern to be modeled, while the third Gaussian is centered. The complete 1D collapse model is given by

$$c(x) = \frac{1}{3\sqrt{2\pi}} \left(\frac{1}{\sigma_1} \kappa_1 \exp\left(-\frac{(x-r_1)^2}{2\sigma_1^2}\right) + \frac{1}{\sigma_2} \kappa_2 \exp\left(-\frac{(x+r_2)^2}{2\sigma_2^2}\right) + \frac{1}{\sigma_3} \kappa_3 \exp\left(-\frac{x^2}{2\sigma_3^2}\right) \right), \quad (3)$$

where r_i represents the offset radii, σ_i represents the standard deviations, and κ_i represents the gains specifying the paint thickness for each Gaussian. Figure 2 shows the composite film build for a parameterization of (3).

Using the 1D collapse model, it is straightforward to determine the thickness variation as the result of multiple passes as shown in Figure 3. The reader is referred to [12] for further details on the calculation of the paint thickness variance.

4 Experimental Validation

The 2D deposition and 1D collapse models were validated by conducting a series of tests in an industrial paint shop. The experiments used an ABB S3 robot with an ABB 50 mm Micro-Micro Bell atomizer attached to apply a solvent based automotive paint to phosphate coated test panels. The operating conditions of the application process were 80-90 kV electrostatic voltage, 150 cc/min paint flow, 250 l/min shaping air flow, and a bell speed of 30 000 RPM. The total film thickness of the oven cured test panels was measured with an Elcometer 355 coating thickness measuring device. Five

measurements were taken for each data point, with the low and high discarded and the average of the remaining three recorded. The average phosphate thickness was then subtracted from the total film thickness to give the paint thickness.

4.1 Deposition Model Parameterization

In order to determine the values for the 1D collapse and 2D deposition model parameters, experimental data was gathered from flat panels painted by three passes as shown in Figure 3. We chose to fit our model to a 577 mm index test, and used numeric optimization to determine the best parameter values for the 1D collapse, which were then used to initialize the 2D model.

Given initial parameter values for the 2D deposition model, we calculated the 1D collapse thickness values from the 2D model using numeric integration. The 1D collapse values were then compared to the experimental data, with numeric optimization used to find the 2D deposition model parameter values that minimized the sum squared error between the experimental data and the numerically integrated 1D collapse. The parameterized models, both 2D and 1D collapse, were shown previously in Figure 2. Figure 4 shows the resulting profile (1D collapse) obtained from a simulation using the 2D deposition model against the experimental data to which it was fit. The simulation results were obtained through numeric evaluation of our deposition models, and give a good match to the experimental data.

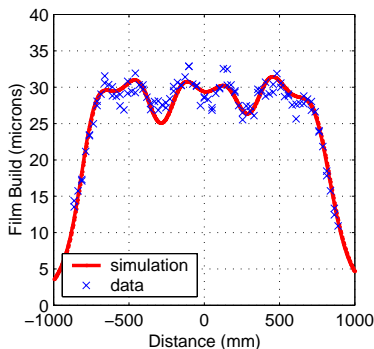


Fig. 4. Flat panel test results using a 577 mm index distance. (avg. error = -0.12 microns, standard deviation = 1.31 microns) The deposition simulation uses triangulated surface elements to model the thickness deposition at a given point on the surface.

4.2 Planar Deposition Results

Using the 2D deposition model parameterized by the 577 mm index three pass test, the depositions generated by 525 and 625 mm index tests were simulated and compared to the experimental data. The results are shown in Figure 5. The model gives a good prediction of both average film build and the structure of the variation for these flat panel tests. Most importantly, the model

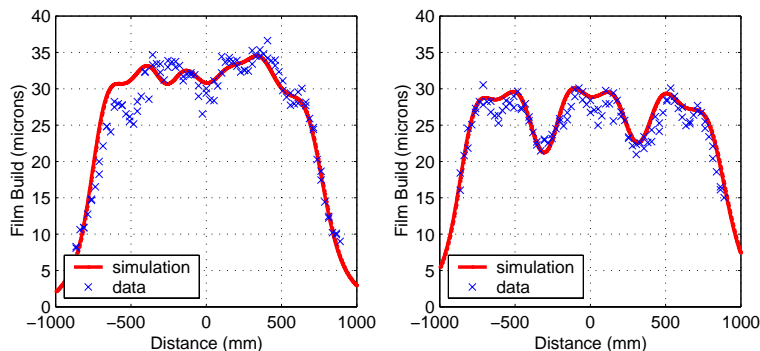


Fig. 5. Flat panel test results: (l) 525 mm index test, and (r) 625 mm index test. Both (l) and (r) used the model parameterized by the data from the 577 mm index test. Both simulations capture the variation due to the structure of the deposition pattern. (average error: l = -0.69 and r = -1.05 microns, standard deviations: l = 2.41 and r = 1.68 microns)

captured both the asymmetries and the structural variation dependence on index distance.

4.3 Surface Deposition Results

Given the relatively good results of the flat panel tests, the projection of the planar deposition model onto arbitrary surfaces was tested. A representative automotive surface was obtained by using a Ford F-150 truck door. Figure 6 shows a CAD model of the truck door used, with an example path shown. The door has a line of convex curvature near the middle, with a pronounced concave curvature on the bottom third of the door. A series of tests were conducted using both horizontal and vertical passes over the door. For the horizontal passes, film build measurements were taken in four vertical columns of data spread across the door, numbered top to bottom. For the vertical passes, the measurements were taken from six rows spread vertically over the door spanning left to right across the door. For the first horizontal test, results for a typical column are shown in Figure 6, which also shows the simulated deposition for each pass individually.

Near the top of the door, in the relatively flat portion, the simulation gives somewhat reasonable results. However, the simulation fails to accurately predict paint thickness in the highly curved section near the bottom of the door. Clearly the pass along the lower portion of the door deposits more paint than the simulation predicts. It is theorized that when the surface curves away from the bell, electrostatic effects dominate invalidating the geometric projection model described in Section 3. Similar tests were conducted for vertical painting motions, with comparable results.

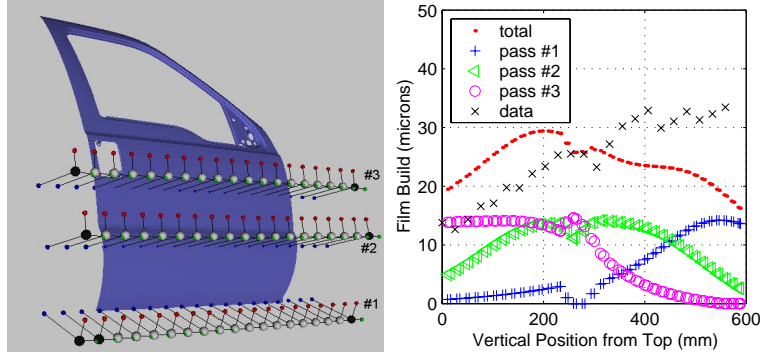


Fig. 6. (l) Door with horizontal paint path shown. The robot paints left to right starting at the left of pass #1, then travels right to left along pass #2, finishing by going left to right along pass #3. (r) Simulation of a horizontal painting motion over the door, with deposition by individual passes shown.

4.4 Miscellaneous Results

It was also desired to verify that our deposition models scale with applicator speed. To this end, two additional tests were conducted. These tests used a single pass, with the robot painting horizontally, at tip speeds of 100 mm/sec and 250 mm/sec. It was intended to compare these results to the 50 mm/sec 3-pass results. The 250 mm/sec test resulted in significant spattering at the nominal paint flow rates being used. Since the sensor was not designed to measure discrete drops of paint, the results were deemed inadmissible. The result for the 100 mm/sec test is shown in Figure 7. As shown, the simulation predicted much greater paint deposition than actually measured. It has been theorized that the transfer efficiencies increase when painting wet surfaces, because some paint initially bounces off of the dry surfaces. Slower tip speeds allow more wet paint film to build up, thereby increasing the average transfer efficiency.

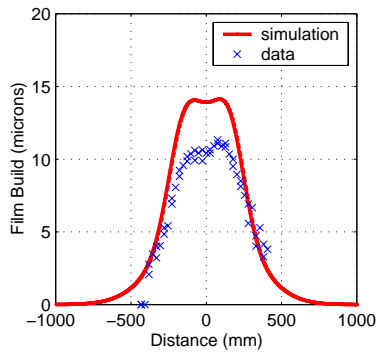


Fig. 7. Single Horizontal pass with $V=100$ mm/sec. Simulation predicts higher paint deposition than data shows for this higher speed, likely due to changes in wet/dry transfer efficiency.

Also notice that the data set in Figure 7 exhibits an asymmetry, while the simulation does not. During this test, the orientation of the atomizer was consistent with the previous 577 3-pass test, while the direction of travel was orthogonal to the 577 mm index test used in the model parameterization. The deposition model developed in Section 3 has a hemispheric asymmetry. This test implies the need for a more localized asymmetry term in the 2D model. Since the 1D collapse model is dependent on the direction of travel anyway, no change to the 1D collapse model is needed. With the addition of this more localized asymmetry component, the model error would need to be calculated against both horizontal and vertical motions during the parameter optimization. The reader is referred to [12] for the development of this modification.

5 Conclusions

The experimental study confirms both the structure of our planar deposition model and the dependence of the thickness variation on that structure. The models we developed accurately predict deposition on planar surfaces, where the atomizer is oriented normal to the surface. Additionally, our analytic 1D collapse model effectively predicts the dependence of the thickness variation on the index distance between passes. Although the experimental results from deposition on the curved surface of the door point to shortcomings with the simple geometric projection developed in Section 3, the experiments do confirm the interaction of the surface curvature with the planar deposition pattern. These preliminary results also indicate the need for additional tests regarding the dependence on the deposition pattern and transfer efficiency on the speed of the atomizer as it moves relative to the surface.

Despite the shortcomings of our 2D deposition model, the models are useful for our research. By using an analytic model, we are able to develop our understanding of the interaction between the surface, the deposition pattern, and the atomizer path. This enables our exploration of path planning techniques that influence overall quality measures such as thickness variation, cycle time, and efficiency. Since the main focus of our research is on path planning, we will continue to use these analytic models during the development phase of our planning tools. Since our planning tools rely only on the structure of the deposition on the surface, and not on the underlying model, the need for more expensive models or experimental data is delayed until the implementation stage.

6 Acknowledgments

This work was supported by the National Science Foundation through grant IIS-9987972 and the Ford Motor Company.

The authors gratefully acknowledge the assistance of the Ford Motor Company and ABB Process Automation for their assistance in conducting the experiments. We would like to specifically acknowledge Dr. Jake Braslaw, our Ford collaborator, who has been extremely helpful throughout this effort.

References

1. Kevin R. J. Ellwood and J. Braslaw. A Finite-Element Model for an Electrostatic Bell Sprayer. *Journal of Electrostatics*, Vol. 45(1), 1998.
2. Alaa A. Elmoursi. Electrical Characterization of Bell-Type Electrostatic Painting Systems. *IEEE Transactions on Industry Applications*, Vol. 28(5), October 1992.
3. Hua Huang and Ming-Chai Lai. Simulation of Spray Transport from Rotary Cup Atomizer using KIVA-3V. In *ICLASS 2000*, Pasadena, California, USA, July 2000.
4. Jacob Braslaw. personal communication, 2001.
5. Suk-Hwan Suh, In-Kee Woo, and Sung-Kee Noh. Development of An Automated Trajectory Planning System (ATPS) for Spray Painting Robots. In *IEEE Int'l. Conf. on Robotics and Automation*, Sacramento, California, USA, April 1991.
6. Naoki Asakawa and Yoshimi Takeuchi. Teachless Spray-Painting of Sculptured Surface by an Industrial Robot. In *IEEE Int'l. Conf. on Robotics and Automation*, Albuquerque, New Mexico, USA, April 1997.
7. Weihua Sheng, Ning Xi, Mumin Song, Yifan Chen, and Perry MacNeille. Automated CAD-Guided Robot Path Planning for Spray Painting of Compound Surfaces. In *IEEE/RSJ Int'l. Conf. on Intelligent Robots and Systems*, 2000.
8. Ramanujam Ramabhadran and John K. Antonio. Fast Solution Techniques for a Class of Optimal Trajectory Planning Problems with Applications to Automated Spray Coating. *IEEE Transactions on Robotics and Automation*, Vol. 13(4), August 1997.
9. Eckhard Freund, Dirk Rokossa, and Jürgen Roßmann. Process-Oriented Approach to an Efficient Off-line Programming of Industrial Robots. In *IECON '98: Proceedings of the 24th Annual Conference of the IEEE Industrial Electronics Society*, volume 1, 1998.
10. M. A. Sahir and Tuna Balkan. Process Modeling, Simulation, and Paint Thickness Measurement for Robotic Spray Painting. *Journal of Robotic Systems*, Vol. 17(9), 2000.
11. Peter Hertling, Lars Høg, Rune Larsen, John W. Perram, and Henrik Gordon Petersen. Task Curve Planning for Painting Robots — Part I: Process Modeling and Calibration. *IEEE Transactions on Robotics and Automation*, Vol. 12(2), April 1996.
12. David C. Conner, Prasad N. Atkar, Alfred A. Rizzi, and Howie Choset. Deposition Modeling for Paint Application on Surfaces Embedded in \mathbb{R}^3 . Technical Report CMU-RI-TR-02-08, Carnegie Mellon, Robotics Institute, Pittsburgh, Pennsylvania, USA, September 2002.